Long-Reach Wavelength-Routed TWDM PON: Technology and Deployment

Liang B. Du, *Member, IEEE*, Xiangjun Zhao, *Member, IEEE*, Shuang Yin, Tao Zhang, *Member, IEEE*, Adam E. T. Barratt, Joy Jiang, Daoyi Wang, Junyan Geng, Claudio DeSanti, and Cedric F. Lam, *Senior Member, IEEE, Fellow, OSA*

***Abstract*—We present a long-reach wavelength-routed time-wavelength division multiplexing (TWDM) passive optical network (PON) architecture (LRWR-PON) and its commercial implementation, which supports up to 768 users per fiber strand and up to 50-km transmission distance. The increased reach allows central offices to become more flexible and fewer in quantity, while the increased aggregation reduces the size and number of optical cables needed, enabling smaller trenches to be used. LRWR-PON also contains eight additional point-to-point wavelengths on each fiber to support wireless sites and/or high-speed dedicated bandwidth applications, greatly simplifying converged network designs. Multiple new optical components and modules have been developed to implement our novel architecture. These include a cyclic arrayed waveguide grating to passively aggregate and distribute access wavelengths in the field, an integrated optical amplifier and multiplexer combination device to aggregate optical line terminal (OLT) channels and extend the system reach, several dense wavelength division multiplexing OLT optics, and a colorless TWDM optical network terminal employing low-cost tunable burst-mode lasers. Our analysis shows the simplification of the civil construction enabled by LRWR-PON greatly outweighs the increased optical component complexity. To date, we have conducted a successful field trial with 606 real-life customers for more than 15 months and we have been rolling out LRWR-PON in Google Fiber markets for production services.**

***Index Terms*—Optical amplifiers, optical planer waveguides, optical receivers, optical transmitters, passive optical networks, time division multi-access, wavelength division multiplexing.**

I. Introduction

CURRENT passive optical network (PON) deployments support limited spatial scalability, as shown in Fig. 1. Specifically, using the typical gigabit-capable PON (GPON) class C+ optics [1], each GPON optical line terminal (OLT) connection supports 64 subscribers over 20 km on a single strand of feeder fiber. Most PONs use time division multiplexing (TDM) with a power splitter at the remote node and all users share the aggregate bandwidth. Although more subscribers are allowed on higher rates PON standards [2], [3], the optical budget greatly limits the possible splitting ratio in all but very short links. For example, both class PR40 in 10G-EPON [4] and class E1 in XGS-PON [2] support 64 subscribers over 20 km. This is due to the fact that the evolution of PON technology has been focused so far on increasing the throughput of PONs to meet the growth of Internet traffic and not to enable more efficient outside plant (OSP) designs. The limited reach and aggregation capability of existing standards requires numerous central offices (COs) to house OLTs in a typical metropolitan area in order to provide adequate coverage in urban and suburban areas. However, COs are expensive and time consuming to build. It is often also very difficult to find suitable locations for new COs because of their external appearance and power feed requirements. Additionally, each CO is associated with a fixed maintenance cost, so more COs result in higher operational costs. Reach extension for TDM PONs by using optical amplification at the OLT has been investigated [5], but has not resulted in widely available commercial products.

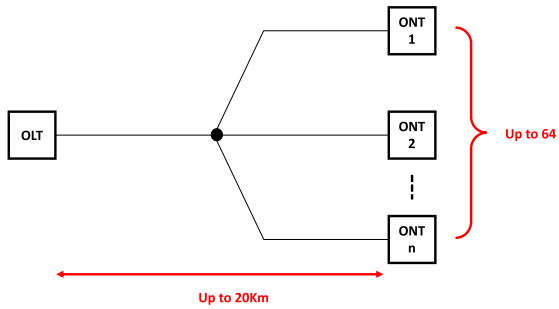

Fig. 1. Example of current PON spatial scalability.

Amplified super-PONs were initially proposed to replicate broadcast signals for a very large number of customers [6]. More recently, bidirectional time-wavelength division multiplexed (TWDM) super-PONs have been proposed as a potential method of centralizing the switching elements to a central location and leaving only optical amplifiers and passive optical components at the remote CO locations [7]–[13]. Most of these have limited the optical distribution network (ODN) to exclusively use power splitters to offer maximum operational flexibility as it allows all users to access all wavelengths [7]–[9]. However, wavelength splitting allows larger total splitting ratios for a given link budget so the combination of wavelength and power splitting allows a larger total splitting ratio than power

Manuscript received December 23, 2017; revised March 20, 2018 and May 22, 2018; accepted June 11, 2018. Date of publication June 25, 2018; date of current version February 21, 2019. *(Corresponding author: Cedric F. Lam.)*

L. B. Du, X. Zhao, S. Yin, T. Zhang, A. E. T. Barratt, J. Jiang, D. Wang, C. DeSanti, and C. F. Lam are with Google Inc., Mountain View, CA 94043 USA (e-mail: clam@google.com).

J. Geng was with Google Inc., Mountain View, CA 94043 USA. She is now with Waymo, Mountain View, CA 94043 USA (e-mail: jgeng@google.com).

Color versions of one or more of the figures in this paper are available online at http://ieeexplore.ieee.org.

Digital Object Identifier 10.1109/JLT.2018.2850343

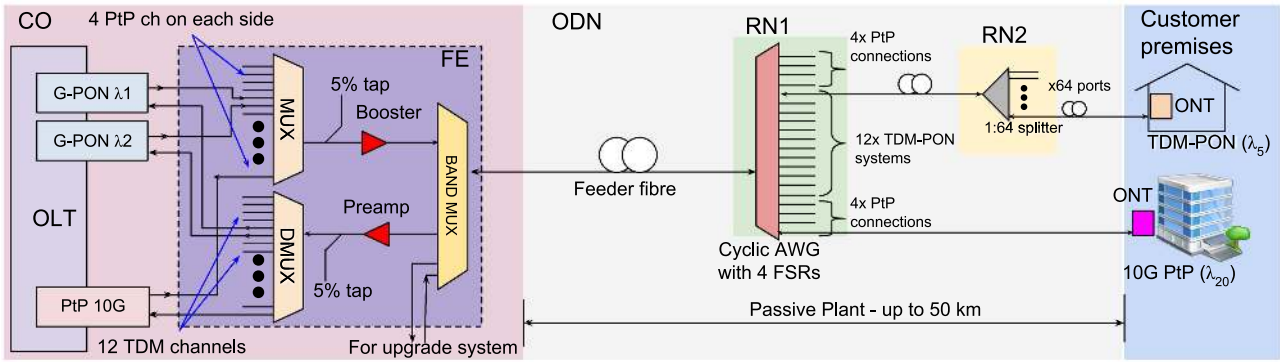

Fig. 2. Architecture of the LRWR-PON System.

splitting alone [11]–[14]. These contributions focus on operational benefits of centralizing the switching equipment and assume the existence of a powered remote CO. Such architectures do not assist deployments where powered structures are difficult to obtain. Architectures using optical amplification at the OLT location have been proposed to reduce the number of powered CO locations needed [15], [16]. High-gain optical amplification is used to enable both a long-reach and high-aggregation. Despite a large body of quality research [17]–[19] and the NG-PON2 standard capturing many of the operational benefits of TWDM super-PONs [20], super-PONs have never been widely deployed commercially. A major limiting factor is the perceived high cost of optical modules.

In this paper we describe a long-reach wavelength-routed TWDM super-PON architecture (LRWR-PON) and its commercial implementation. Each strand of fiber can support up to 768 TDM terminals, mostly for residential users, and 8 point-to-point (PtP) terminals, for business users and wireless x-haul, at a reach of 50 km [22]. This super-PON system was developed to reduce deployment costs of "greenfield" network builds and requires no powered sites between the CO housing OLTs and the subscribers. We worked closely with optical module vendors to make sure the developed equipment could meet the very tight cost constraints of access networks. The system level requirements were developed with key technology partners to balance the system capabilities against the complexity and cost of critical components, such as the optical network terminal (ONT). This collaborative effort has yielded a low cost TWDM super-PON system suitable for residential, business, and wireless applications.

LRWR-PON differs from the most common NG-PON2 configuration in two ways: (1) uses wavelength and power splitters instead of only power splitters in the ODN; (2) uses optical amplification inside the CO. These changes allowed the removal of the tunable optical filter from the ONT receiver, higher minimum side-mode suppression ratio (SMSR) and lower output power for the ONT and OLT transmitters. These relaxations simplify the optical components, which have been the largest challenge in realization of NG-PON2 [21]. The NG-PON2 flexibility of having all wavelengths at all terminals is exchanged for simpler and lower cost optical components in LRWR-PON.

We have completed the development of a LRWR-PON system based on the GPON TC layer, using standard GPON OLTs, standard GPON ONT chipsets, and modified optical modules.

A trial system with 606 live customers in Palo Alto, California was constructed between December 2016 and March 2017. At the time of writing, zero physical layer issues were reported after 15 months of live customers. Google Fiber is now deploying the LRWR-PON system in production markets. The centralization of active network electronics enabled by LRWR-PON has resulted in faster and more predictable deployment speeds. We are now in the development phase of a subsequent, higher rate system.

II. System Architecture

The system architecture is shown in Fig. 2. The required long reach and large split ratio means some form of optical amplification is needed. Previous studies have shown that erbium-doped fiber amplifiers (EDFA) are most effective for amplifiers co-located with OLTs [23]. To enable the use of mature EDFA technology [24], the upstream wavelengths are confined to the C-band and the downstream wavelengths are confined to the L-band. Nominally 100-GHz channel spacing is used to balance the required tuning range of colorless ONTs and to operate lasers without external wavelength lockers. Two sub-bands are required in the upstream and downstream spectrum to enable the coexistence of two system generations. Therefore, the 44 100-GHz channels within the C-band are grouped into two sub-bands, with 22 channels in each one. The two edge channels in each sub-band are reserved as guard-bands between the bands, to allow for separation of the bands, and are not used. The channels available in each sub-band are therefore 20. The channel allocation for the 4 sub-bands is shown in Fig. 3(a). The four channels on each side are used for PtP services, at the speed of 10 Gb/s for the current generation, to support businesses, wireless x-haul, or uplinks for an operator's internal networking equipment. The central 12 channels are used for TDM services, to serve mostly residential customers, because they have lower losses through the CAWG [28], critical for TDM-PONs because of the subsequent lossy power splitter. TWDM ONTs are mass deployed, so colorless ONTs are needed to minimize operational complexity. The current generation operates at

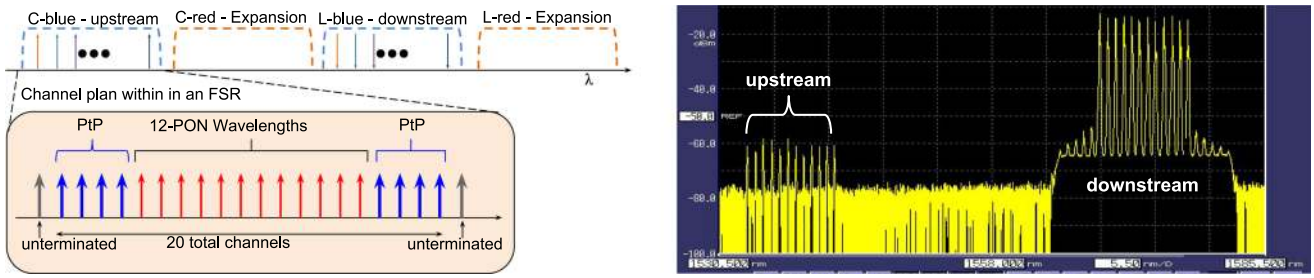

(a) (b)

Fig. 3. (a) Wavelength plan of LRWR-PON; (b) OSA trace of combined downstream and upstream LRWR-PON system with 12 TDM channels.

2.5 Gb/s downstream and 1.25 Gb/s upstream; the subsequent generation system will operate at 10 Gb/s or greater. Fig. 3(b) shows the optical spectrum of the 12 downstream and upstream TDM channels for the current system. The upstream and downstream tap ports from the FE were combined using a 50/50 optical coupler to generate the signal into the optical spectrum analyzer. It is possible to reconfigure the ratio of PtP and TDM channels in actual network deployments.

The TDM channels in LRWR-PON are logically independent from each other, which makes the upper layer protocols compatible with the transmission convergence (TC) layer of GPON, XG-PON, and XGS-PON, or the physical coding sublayer (PCS) and physical medium attachment (PMA) sublayers of EPON and 10G-EPON. It is therefore possible to construct a LRWR-PON system using existing commercial OLTs with modified optical modules to gain a 12 times increase in the aggregated bandwidth and the maximum number of users per fiber, relative to the underlying standard. The TDM channels in LRWR-PON use the GPON TC layer [26], enabling the use of commercial GPON OLT systems with minimal integration effort. The ranging wait time was increased to allow enough time for ONTs 50 km away to range. The wavelength channel information is carried in the broadcast PON_ID PLOAMd message, detailed in Annex C of [26], which is an optional GPON protocol overhead field. The PON_ID PLOAMd message is sent approximately once per second. Each ONT listens for its assigned wavelength in the PON_ID message, and tunes to that wavelength. The ONT then ranges as per the GPON standard [26]. Once ranged, the ONT wavelength is never changed.

The TDM OLT transmitters consist of fixed-wavelength dense wavelength division multiplexing (DWDM) directly modulated distributed feedback (DFB) lasers. The receivers are unfiltered burst-mode avalanche photodiodes (APD). Duplex fiber interfaces are used on the OLT optics to keep the downstream/upstream multiplexer/demultiplexer separate, as shown in Fig. 2. 20-channel arrayed waveguide gratings (AWG) are used as a multiplexer and a demultiplexer. A booster EDFA amplifies the multiplexed downstream signal; a preamplifier EDFA amplifies the combined upstream signal. The relatively high cost of EDFAs is shared among hundreds of users. A thin-film filter (TFF) based band-multiplexer (BM) combines the upstream and downstream signals into a bidirectional signal. Two additional ports on the BM are reserved for the expansion bands, to enable the seamless insertion of a future generation system. This is similar to pre-installing the WDM coexistence filter for upgrading GPON [25] to allow the seamless insertion of a future generation system. Integrated tap ports are provided to allow balancing of the individual channels, if needed.

The first stage of splitting occurs inside the first remote node (RN1). A cyclic AWG (CAWG) is used to separate the different channels within each band. The CAWG has a free-spectral range (FSR) of 22 channels, with 20 terminated ports, matching the channel plan shown in Fig. 3(a). The first CAWG output port passes the first channel from each of the four sub-bands, the second port passes the second channel from each of the four sub-bands, and so on. A 20-port CAWG has significantly lower loss than a 20-port splitter, thereby greatly reducing the required link budget. The wavelengths received by each customer are determined by which CAWG port the customer is attached to. All future system generations on this ODN have to use the wavelength plan shown in Fig. 3(a) with nominally 100-GHz channels.

In the second remote node (RN2), a power splitter is used to split each TDM channel. A 64-way power split, for example, enables up to 768 TDM users per fiber strand (12×64). The optical link budget is designed for 50-km reach with a 64-way power split, which allows the use of one or very few centralized OLT locations to serve most metropolitan areas. The ability to support 768 users per fiber strand provides sufficient aggregation to allow very large COs to be connected using thin fiber cables in small micro-trenches.

In the ONT, a directly-modulated distributed Bragg reflector (DBR) laser is used to enable tuning across the 12 TDM channels. The manufacturing cost of the tunable ONT is kept low by limiting the tuning range to 12 channels and by requiring a low output power of 0 dBm. Additionally, the wavelength selectivity of the CAWG relaxes the SMSR requirements and the allowed light levels from the TWDM ONT transmitter during burst-off times because any light outside of the assigned channel is removed by the CAWG prior to entering the feeder fiber. The narrow-band, tunable filter required in an NG-PON2 ONT is removed and replaced in a TRWR-PON ONT by a broadband optical filter integrated into a common bidirectional optical subassembly (BOSA). These relaxations have allowed the creation of a low-cost colorless ONT.

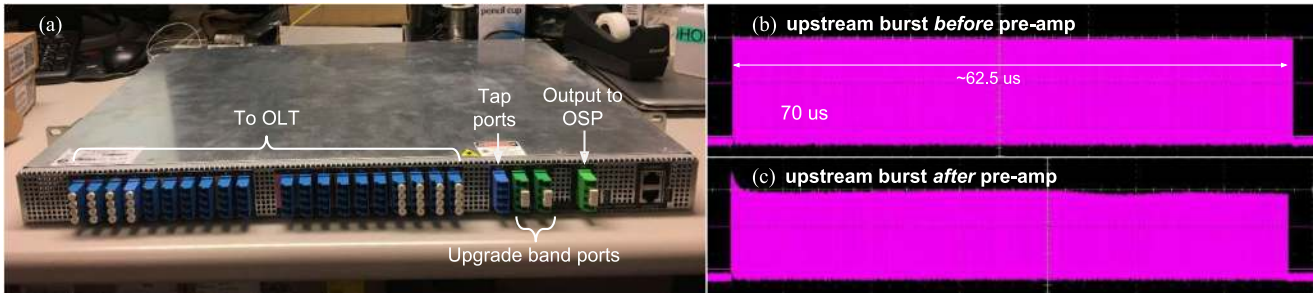

(a) (b)

Fig. 4. (a) Photo of the FE; (b) Upstream time-domain waveform before pre-amplifier; (c) Upstream time-domain waveform after pre-amplifier.

TABLE I
OPTICAL BUDGET CALCULATION

Component	Count	unit loss [dB]	Total loss [dB]
CAWG	1	5.5	5.5
Power splitter(s): 64-way total	1	20.5	20.5
Fiber	50	0.22	11
Connectors	4	0.25	1
Splices	20	0.05	1
Margin	1	3	3
Total Loss			**42**

Note: Margin accounts for any transmission impairments, power imbalance between WDM channels, and unexpected losses from field work.

III. System Design and Testing

A. Optical Budget Requirement

The loss elements for a typical 50 km access link are shown in Table I. This table only includes elements in the ODN between the CO and the user, it does not include optical components within the CO. The system reach is specified from the last CO to the user, with no optical amplification.

B. Fiber Expander (FE)

To optimize for space and deployment simplicity, the multiplexer/demultiplexer, amplifiers, and BM for two systems are packaged into a single 23-inch 1 rack unit high (1.75-inches) rack-mountable unit, as shown in Fig. 4(a).

In the downstream direction, an L-band booster EDFA is used to amplify the multiplexed downstream signals from the OLT(s). Assuming ONT receiver sensitivity of -32 dBm with forward error correction (FEC), as described in Section III-E, a launch power of 10 dBm per channel is required for the downstream TDM signals. The booster EDFA is specified to have a total composite output power of 24 dBm at the output of the FE, which supports up to 12 TDM channels at $+13$ dBm per channel and 8 PtP channels at $+3$ dBm per channel, allowing for a 3 dB variation in the powers of different wavelength channels. The PtP channels do not pass through power splitter(s), meaning $\sim$20 dB lower link loss. A 10 dB lower launch power is used to balance saving power for the TDM channels and allowing sufficient power in the PtP channels to operate at 10 Gb/s without FEC.

Because of the high power, a backscattering detector is incorporated to detect fiber cuts. Detection of a fiber cut triggers an automatic reduction in the downstream launch power to below 21.5 dBm, below the limit of class 1M. In a healthy plant ONT ports only receive one channel, which is less than the class 1 limit of 10 dBm.

In the upstream direction, a gain-clamped C-band preamplifier is used for the burst-mode upstream signals to avoid burst length dependent gain fluctuations [27]. The total small-signal gain of the FE unit is 14.5 dB, to allow a 0-dBm ONT launch power. The effective noise figure (NF) of the FE in the upstream direction is 7.5 dB, which includes a $\sim$2-dB input loss from the BM.

To quantify the effectiveness of the gain clamping, the signals at the EDFA's input (Fig. 4(b)) and output (Fig. 4(c)) were measured. The input power was measured to be -8 dBm, which is 11 dB higher than the specified maximum input power per wavelength channel and is equivalent to the extreme worst case of all 12 channels having a synchronized burst. The short increase in power at the start of the burst is created by transient effects of the EDFA. The time constant is determined by the gain feedback loop of the EDFA's gain clamping mechanism. The total gain excursion of $<$1.2 dB was measured for this very extreme case. Reducing the input power by 6 dB allowed the gain excursion to be reduced to 0.5 dB, which produces negligible sensitivity penalty.

C. Cyclic AWG (CAWG)

The detailed LRWR-PON wavelength plan is shown in Table II and contains four FSRs, which are nominally 100-GHz spaced. The exact channel spacing is slightly reduced for longer wavelength FSRs due to dispersion inside the waveguides of the CAWG. The central 12 channels for TDM services are highlighted in orange. Fig. 5(a) shows the plot of the wavelength response of the CAWG at room temperature, showing 4 FSRs. The center channels of each FSR have $<$5-dB attenuation. At the edges of each FSR, the attenuation increases by $\sim$0.5 dB, which is as expected [28].

The CAWG is designed to be athermal to enable use in an outdoor environment. The wavelength shift for each channel at

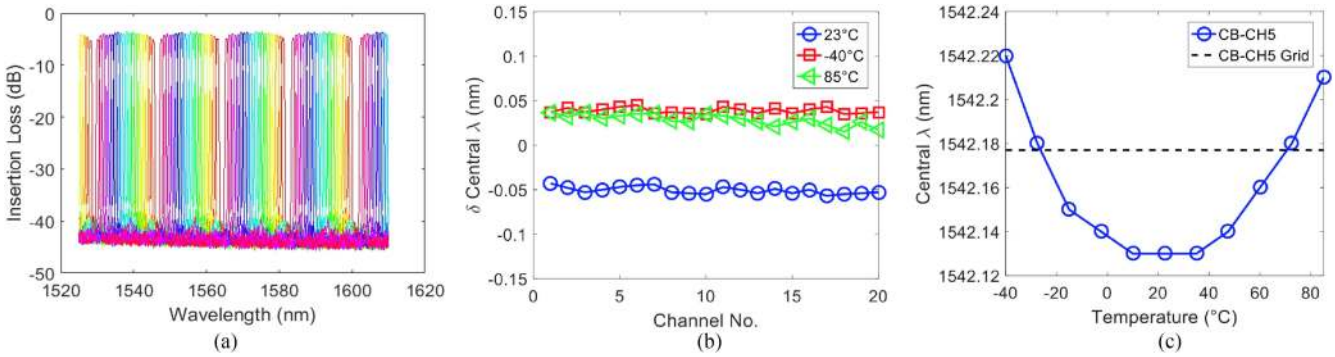

Fig. 5. (a) Cyclic wavelength response of CAWG with each port shown as a different color; (b) Wavelength shift for the C-blue band at three temperatures; (c) Wavelength shift against temperature for channel X of the C-blue band.

TABLE II
WAVELENGTH PLAN OF THE LRWR-PON SYSTEM

	C-band Blue (C-B) Upstream		L-band Blue (L-B) Downstream		C-Band Red (C-R) Upstream		L-band Red (L-R) Downstream	
Ch #	Freq (GHz)	WL (nm)	Freq (GHz)	WL (nm)	Freq (GHz)	WL (nm)	Freq (GHz)	WL (nm)
1	193.991	1545.39	189.609	1581.11	191.800	1563.05	187.418	1599.59
2	194.092	1544.59	189.708	1580.29	191.900	1562.23	187.516	1598.76
3	194.193	1543.78	189.807	1579.46	192.000	1561.42	187.613	1597.93
4	194.294	1542.98	189.906	1578.64	192.100	1560.61	187.711	1597.10
5	194.396	1542.18	190.004	1577.82	192.200	1559.79	187.809	1596.27
6	194.497	1541.38	190.103	1577.00	192.300	1558.98	187.906	1595.44
7	194.598	1540.57	190.202	1576.18	192.400	1558.17	188.004	1594.61
8	194.699	1539.77	190.301	1575.36	192.500	1557.36	188.102	1593.78
9	194.800	1538.97	190.400	1574.54	192.600	1556.56	188.200	1592.95
10	194.901	1538.18	190.499	1573.73	192.700	1555.75	188.297	1592.12
11	195.003	1537.38	190.597	1572.91	192.800	1554.94	188.395	1591.30
12	195.104	1536.58	190.696	1572.09	192.900	1554.13	188.493	1590.47
13	195.205	1535.78	190.795	1571.28	193.000	1553.33	188.590	1589.65
14	195.306	1534.99	190.894	1570.47	193.100	1552.52	188.688	1588.83
15	195.407	1534.19	190.993	1569.65	193.200	1551.72	188.786	1588.00
16	195.508	1533.40	191.092	1568.84	193.300	1550.92	188.883	1587.18
17	195.609	1532.61	191.191	1568.03	193.400	1550.12	188.981	1586.36
18	195.711	1531.82	191.289	1567.22	193.500	1549.32	189.079	1585.54
19	195.812	1531.02	191.388	1566.41	193.600	1548.52	189.176	1584.72
20	195.913	1530.23	191.487	1565.60	193.700	1547.72	189.274	1583.91

three temperatures is shown in Fig. 5(b). The wavelength shift of this unit was $\sim\pm 0.05$ nm for all channels at the tested temperatures. Fig. 5(c) shows the wavelength shift against temperature for channel 5 in the C-blue band. The wavelength shift has a parabolic shape because the athermalization method compensates for the linear temperature dependence, leaving only the second order temperature-dependent effects [29].

D. OLT Optical Transceivers

OLT transceivers are housed in duplex-fiber small form pluggable (SFP) modules, which are also color coded in their package, as shown in Fig. 6(a). The upstream and downstream signals are kept separate for amplification in the FE, as described in Section II. The transmitter consists of a directly modulated L-band DFB laser with a thermoelectric cooler (TEC). The required output power is -2 dBm; the low output power offsets some of the power consumed by the TEC. This relaxed output power is made possible by the use of the booster EDFA within the FE.

A wideband burst-mode avalanche photodiode (APD) is used to receive the amplified, filtered 1.25-Gb/s upstream signals. Fig. 6(b) shows the upstream bit error ratio (BER) for 12-wavelength (channel 9 measured) back-to-back (B2B) and 50-km systems, with and without the pre-amplifier. The ONT transmitter is working in burst mode with 50% duty-cycle and carrying PRBS23. The burst-mode pre-amplifier improves the sensitivity from -35 dBm to -44 dBm for a target BER of 1.0×10^{-4}, which is the threshold for the optional Reed Solomon (RS) (255, 239) forward error correction (FEC) for GPON. The required ONT launch power is >0 dBm and the required receiver sensitivity at the OLT is -42 dBm, achieving a link budget of 42 dB. Therefore, the measured receiver sensitivity is 2-dB better than our requirement. These tests did not consider any potential degradation to the sensitivity caused by a preceding loud ONT.

E. ONT Optical Transceivers

The ONT box is shown in Fig. 7(a). It includes a slightly enlarged small form factor (SFF) optical module, shown in Fig. 7(b). The ONT SFF module comprises a BOSA. The receiver optical subassembly (ROSA) comprises a 2.5-Gb/s continuous-mode APD. Improvements in the manufacturing process of APDs and transimpedance amplifiers (TIA) allowed the use of an ONT sensitivity of -32 dB at a BER of 10^{-4} for operation with FEC, 2-dB lower than the GPON C+ standard [1]. Fig. 7(c) shows the downstream 2.5-Gb/s BER B2B and through 50 km for the full system (channel 9 measured), with and without the booster EDFA. No penalty was observed for 50-km transmission without booster, suggesting there is little penalty from chromatic dispersion (CD). About 0.8-dB penalty was observed for 50 km with booster, which is due to fiber nonlinearity generated by the $\sim$13-dBm/wavelength launch power. Despite this penalty, a sensitivity of -37.5 dBm at a BER of 1×10^{-4} was observed. Our assumed minimum downstream launch power was 10 dBm, allowing for any channel to be 3 dB lower than the average. Potential contributors to channel power imbalance include OLT transmit power variation, EDFA gain variation, and multiplexer port variations. This particular sample is 5.5 dB better than our -32-dBm requirement.

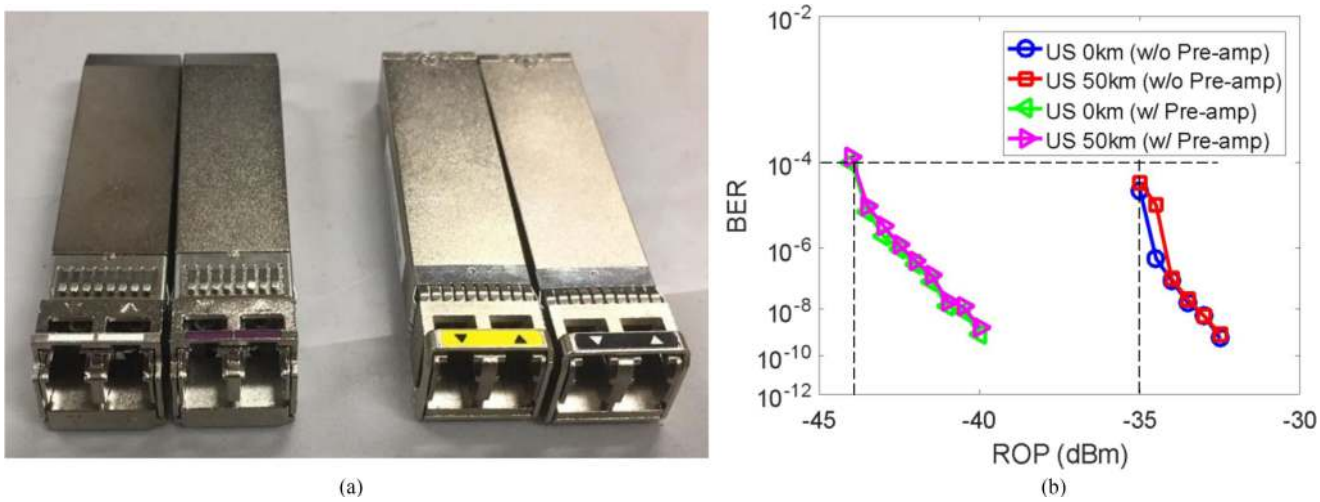

Fig. 6. (a) Photo of color-coded OLT optics; (b) Sensitivity of OLT receiver with and without pre-amplification. ROP – Received Optical Power.

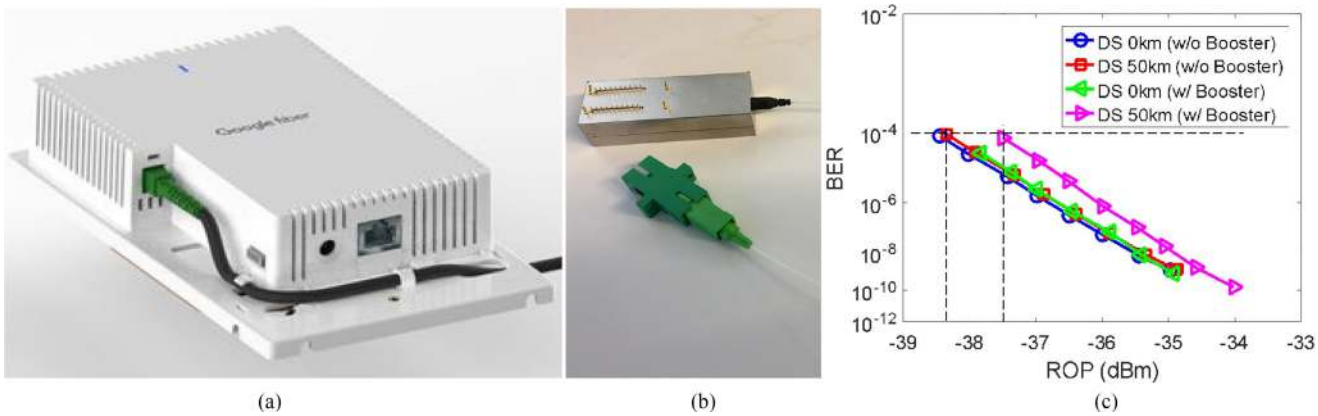

Fig. 7. (a) Photo of ONT; (b) Photo of ONT optical module; (c) Sensitivity of ONT receiver. ROP – Received Optical Power.

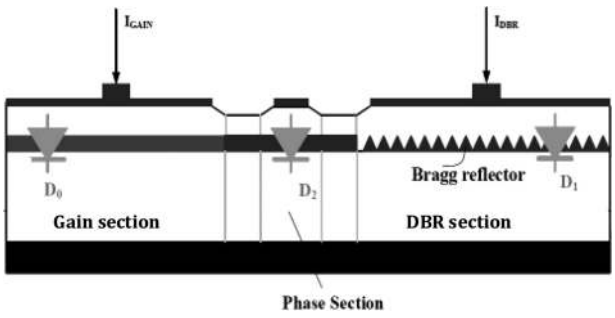

Fig. 8. Diagram of directly modulated DBR laser diode.

The transmitter optical subassembly (TOSA) consists of a directly modulated DBR laser. Fig. 8 shows the structure of the DBR laser. The output wavelength of the DBR can be tuned by over 10 nm by adjusting the DBR injection current. The TEC is used to fine-tune the laser's wavelength. To maximize the output power, light is emitted from the gain section side [30]. The monolithic laser chip and TEC are placed inside a transistor outline can (TO-can), which is the most cost-effective hermetically-sealed optical package.

The difficulty of maintaining wavelength stability due to the self-heating effect in burst-mode DWDM transmitters has been well researched [31]. We reduced the self-heating effect by maintaining a sub-threshold current through the DBR laser's gain section during the "burst-off" period, thereby reducing the change in current through the laser. The lower transmit power also helps to reduce the wavelength shifts. The setup shown in Fig. 9 was used to test the wavelength stability of ONTs. A programmable optical filter was set to have a 50 GHz Gaussian profile with the center wavelength detuned from the ONT's continuous-mode wavelength by ∼25 GHz, thereby attenuating the continuous-mode output signal by ∼3 dB. Any wavelength shifts in the ONT's output is translated to intensity fluctuations by the Gaussian filter in a deterministic manner. The filtered ONT output signal was converted to a photocurrent using a PIN photodiode and captured using a real-time oscilloscope. The envelope of the captured waveform was used to calculate the received optical power against time within a burst. The instantaneous wavelength shift is them calculated from the optical power using a Gaussian relationship. Fig. 9(a) shows the captured waveform with the programmable optical filter set to all-pass, showing the ONT does not produce intensity fluctuations

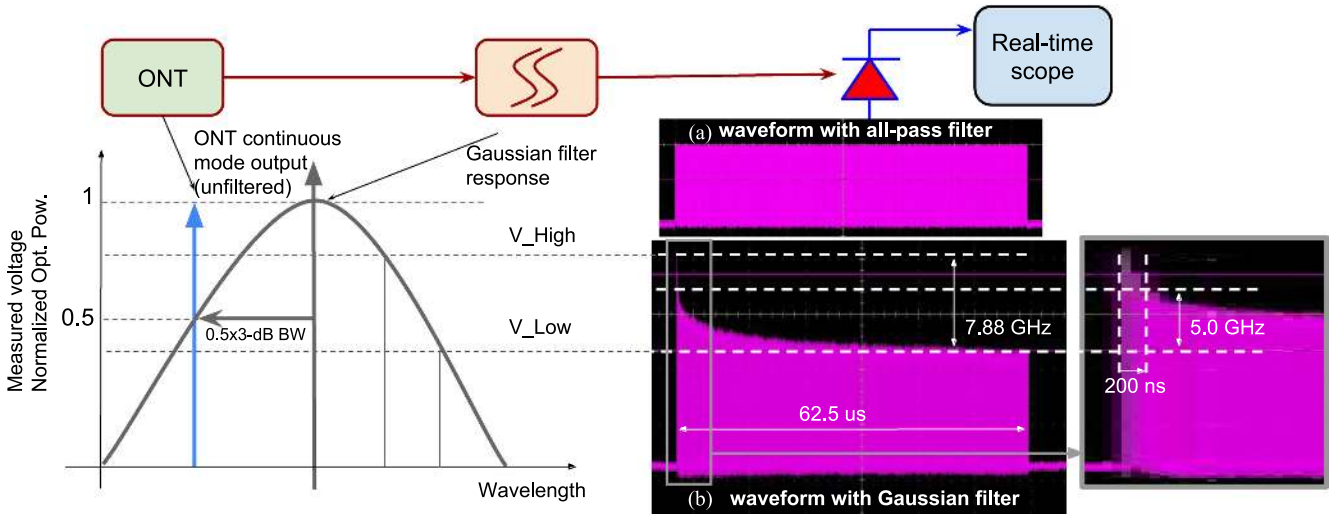

Fig. 9. Setup and results for ONT wavelength drift test.

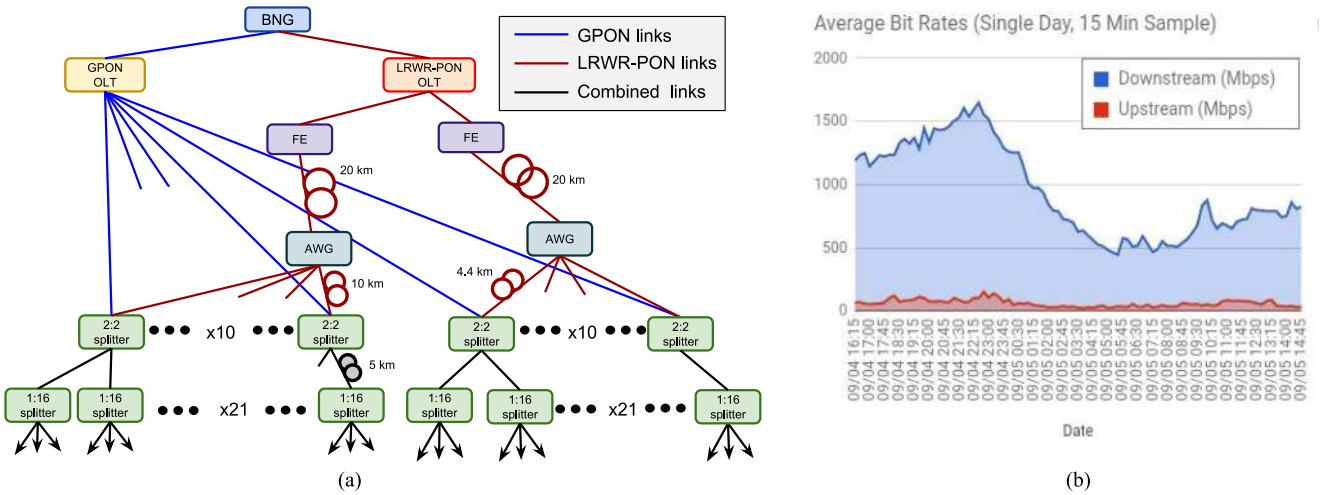

Fig. 10. (a) Stanford trial GPON to LRWR-PON migration setup; (b) Instantaneous total bitrates for the Stanford 606 household trial area.

during the start of the burst. Fig. 9(b) shows the frequency-shift induced intensity fluctuations. The total wavelength shift within a 62.5-μs burst (50% duty cycle of a GPON frame) was measured to be 7.88 GHz. The wavelength shifts rapidly in the first 200 ns. A wavelength shift of <5 GHz was observed from the 200 ns mark to the end of the pulse.

In normal operation, the CAWG's response is aligned to the ONTs wavelength. Therefore, the wavelength to intensity conversion does not occur due to the flat-top response of the CAWG; these power fluctuations are not present when the upstream signal is detected by the OLT.

IV. Field Trial Results

A field trial was started in November 2016 in our Stanford real-life test network covering 606 customers. This test area serves real customers with both unicast data and multicast video services. The trial customers were originally served using standard GPON equipment. Spools of optical fiber were added to the transmission path to extend the distance between the OLT and ONTs to be between 20 and 35 km. To avoid creating any customer outage time during the install period of the trial, both TWDM PON system and standard GPON signals were multiplexed and delivered to all customers using a new layer of 2:2 optical splitters during a transition period of four months. This is possible because the LRWR-PON wavelengths and GPON wavelengths are completely separate so they can easily co-exist. Fig. 10(a) shows the trial setup.

A low-power version of the FE was used, with a maximum output power of 21 dBm. This is below the 1M laser class limit of 21.5 dBm, thus avoiding the need for the auto power-down mechanism. Our plan is to use this lower power version for deployments spanning less than 35 km.

During this four-month period, all GPON ONTs in customers' homes were swapped for LRWR-PON ONTs. As of March 2017, the GPON ONTs were completely swapped out of the trial area, the standard GPON OLT systems were removed, and the additional 2:2 splitters were left intact.

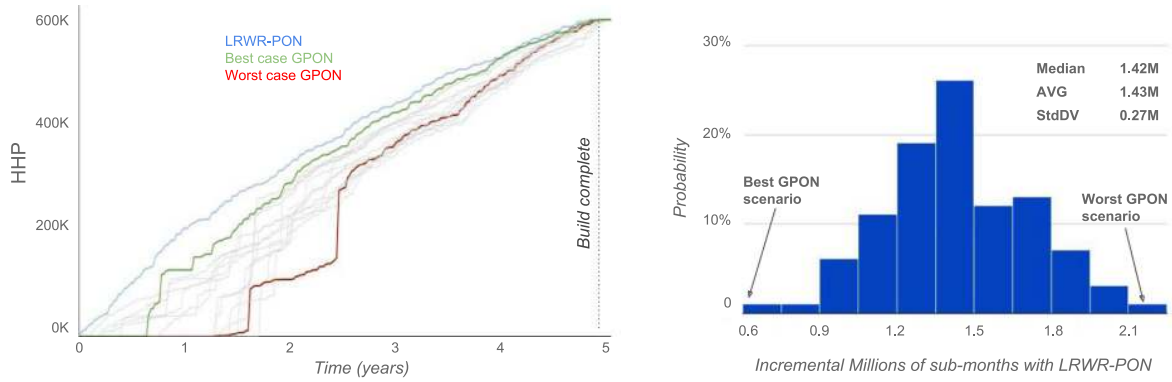

Fig. 11. (a) Number of fully connected households against time; (b) The number of subscriber months brought forward by LRWR-PON compared to GPON.

Fig. 10(b) shows the total instantaneous (15-minute samples) unicast traffic for the 606 trial customers for a 24-hour period on 04/05 September 2017. This data shows that the traffic in Stanford is highly asymmetric, with ∼10 times more downstream traffic than upstream traffic. The peak downstream aggregated traffic observed for that day was ∼1.7 Gb/s. These traffic patterns are representative of the greater Google Fiber network, which is a driving factor for the choice of using 2.5/1.25-Gb/s GPON rates in the first-generation system. We anticipate the next generation system will be at least 10 Gb/s, potentially greater.

V. OSP Design and Deployment

The 2.5-fold increase in reach (compared to GPON with C+ optics at 64-way split) and 12-fold increase in aggregation ratio allows COs to house 6 times more OLT ports and use half as many lit fiber strands exiting the CO. Obtaining suitable locations for CO placement is complex and time-consuming because COs require a high-capacity electrical circuit and are typically unsightly (large air-conditioning structures with no windows), making it difficult to place them in the residential areas where they are needed. Each CO also needs to be actively monitored during operations and maintained on a regular basis. Reducing the required number of COs simplifies operations and deployment.

Statistics were collected on the average turn up times of COs placed in Google Fiber's network from 2013 to 2016. These statistics were then used to create a Monte-Carlo simulation of a 560,000-household metropolitan deployment, comparing the turn up of households using traditional GPON and new LRWR-PON architectures. The GPON deployment assumed 12 Google-constructed COs and two COs in co-locations. The LRWR-PON deployment assumed only the two co-locations for COs. The process to build all Google-constructed COs and the OSP was started on day 1 of the OSP build; the time needed to complete each CO was randomly generated based on statistics of previous Google Fiber CO permitting and construction times. The COs in co-locations were assumed to be available from day 1.

Fig. 11(a) shows the turn up of households as a function of time for the two architectures. The LRWR-PON architecture is only gated by completing the OSP. The GPON architecture also requires OSP completion and serving CO completion to turn up households. Adding serving CO completion as a gating factor greatly affects the turn up of households.

Fig. 11(b) shows the incremental subscriber months enabled by the 2-colocation only physical network architecture. In the best GPON scenario, the CO turnover dates are roughly aligned with the completion of the OSP sections, minimizing the idle time of completed OSP. Even in this very optimistic case, the model still estimates a cost of 0.5 million subscriber months caused by CO turn up. The most likely outcome is around 1.4 million subscriber months are forgone due to waiting for CO turn up. This equates to tens to hundreds of millions of dollars of lost revenue because the completed OSP is waiting the turn up of COs.

VI. Conclusion

At Google Fiber, we successfully developed and deployed LRWR-PON, a 20-channel TWDM Super-PON system with a default configuration of 12 wavelength-overlaid TDM GPON channels and 8 wavelength-overlaid 10-Gb/s PtP channels on a single fiber strand. This system has 50-km reach with 1:64 per-wavelength power-splitting ratio for the TDM channels, equating to 768 TDM PON customers on a single strand.

The key architectural components of the LRWR-PON system were carefully considered, as detailed in Section III, focusing on minimizing the total system cost for a large-scale, residential-dominated deployment. For example, the use of an athermal CAWG at the RN allowed increased reach and eliminated the narrow-band filter from the ONT, reducing ONT costs. The LRWR-PON architecture requires significantly fewer COs and enables use of thinner optical cables, which greatly reduces the deployment and operation costs of fiber to the home networks. Monte-Carlo simulations showed LRWR-PON also enables earlier initiation of subscribers.

Customers have been served using LRWR-PON in our Stanford trial network since November 2016. The number of customer service calls did not increase after the replacement of the standard GPON equipment with the LRWR-PON system. Google Fiber is now deploying LRWR-PON into production markets.

We now aim at standardizing the LRWR-PON architecture to create an industry-wide ecosystem of components. We began activity in both IEEE 802.3 (the EPON protocols standard body) and ITU-T Q2/SG15 (the GPON protocols standard body).

REFERENCES

[1] G.984.2 amendment 2: Gigabit-capable passive optical networks (G-PON): Physical media dependent (PMD) layer specification, New Appendix V, 2008.

[2] G.9807.1: 10-gigabit-capable symmetric passive optical network (XGS-PON), 2016.

[3] *IEEE Standard for Information Technology—Local and Metropolitan Area Networks—Specific Requirements—Part 3: CSMA/CD Access Method and Physical Layer Specifications Amendment 1: Physical Layer Specifications and Management Parameters for 10 Gb/s Passive Optical Networks*, IEEE Std. 802.3av, 2009.

[4] *IEEE Standard for Ethernet - Amendment 1: Physical Layer Specifications and Management Parameters for Extended Ethernet Passive Optical Networks*, IEEE Std. 802.3bk, 2013.

[5] J. Sugawa and H. Ikeda, "Development of OLT using semiconductor optical amplifiers as booster and preamplifier for loss-budget extension in 10.3-Gb/s PON system," in *Proc. OFC/NFOEC*, Los Angeles, CA, USA, 2012, Paper OTh4G.4.

[6] A. M. Hill *et al.*, "39.5 million-way WDM broadcast network employing two stages of erbium-doped fibre amplifiers," *Electron. Lett.*, vol. 26, no. 22, pp. 1882–1884, 1990.

[7] M. Ruffini *et al.*, "DISCUS: An end-to-end solution for ubiquitous broadband optical access," *IEEE Commun. Mag.*, vol. 52, no. 2, pp. S24–S32, Feb. 2014.

[8] K. Taguchi *et al.*, "Field trial of long-reach and high-splitting wavelength-tunable TWDM-PON," *J. Lightw. Technol.*, vol. 34, no. 1, pp. 213–221, Jan. 2016.

[9] I. V. de Voorde, C. M. Martin, I. Vandewege, and X. Z. Oiu, "The super-PON demonstrator: An exploration of possible evolution paths for optical access networks," *IEEE Commun. Mag.*, vol. 38, no. 2, pp. 74–82, Feb. 2000.

[10] D. P. Shea and J. E. Mitchell, "Long-reach optical access technologies," *IEEE Netw.*, vol. 21, no. 5, pp. 5–11, Sep. 2007.

[11] G. Talli and P. D. Townsend, "Hybrid DWDM-TDM long-reach PON for next-generation optical access," *J. Lightw. Technol.*, vol. 24, no. 7, pp. 2827–2834, Jul. 2006.

[12] C. Antony *et al.*, "Upstream burst-mode operation of a 100km reach, 16x512 split hybrid DWDM-TDM PON using tuneable external cavity lasers at the ONU-side," in *Proc. 35th Eur. Conf. Opt. Commun.*, 2009, pp. 1–2.

[13] S. Smolorz *et al.*, "Next generation access networks: PIEMAN and beyond," in *Proc. Int. Conf. Photon. Switching*, 2009, pp. 1–4.

[14] P. P. Iannone *et al.*, "Bi-directionally amplified extended reach 40Gb/s CWDM-TDM PON with burst-mode upstream transmission," in *Proc. Opt. Fiber Commun. Conf. Expo. Nat. Fiber Opt. Eng. Conf.*, 2011, pp. 1–3.

[15] E. Wong, M. Muller, and M. C. Amann, "Colourless operation of short-cavity VCSELs in C-minus band for TWDM-PONs," *Electron. Lett.*, vol. 49, no. 4, pp. 282–284, 2013.

[16] Z. Li *et al.*, "Symmetric 40-Gb/s, 100-km passive reach TWDM-PON with 53-dB loss budget," *J. Lightw. Technol.*, vol. 32, no. 21, pp. 3389–3396, Nov. 2014.

[17] D. B. Payne and R. P. Davey, "The future of fibre access systems?" *BT Technol. J.*, vol. 20, no. 4, pp. 104–114, Oct. 2002.

[18] F. Effenberger *et al.*, "An introduction to PON technologies [Topics in Optical Communications]," *IEEE Commun. Mag.*, vol. 45, no. 3, pp. S17–S25, Mar. 2007.

[19] P. P. Iannone and K. C. Reichmann, "Optical access beyond 10 Gb/s PON," in *Proc. 36th Eur. Conf. Exhib. Opt. Commun.*, 2010, pp. 1–5.

[20] G.989.1: 40-Gigabit-capable passive optical networks (NG-PON2): General requirements, 2013.

[21] R. Bonk *et al.*, "The underestimated challenges of burst-mode WDM transmission in TWDM-PON," *Opt. Fiber Technol.*, vol. 26, pp. 59–70, 2015.

[22] X. Zhao *et al.*, "Long-reach TWDM PON for fixed-line wireless convergence," in *Proc. Eur. Conf. Opt. Commun.*, Gothenburg, Sweden, 2017, Paper W.3.D.2.

[23] N. Genay, P. Chanclou, F. Saliou, Q. Liu, T. Soret, and L. Guillo, "Solutions for budget increase for the next generation optical access network," in *Proc. 9th Int. Conf. Transparent Opt. Netw.*, Rome, Italy, 2007, pp. 317–320.

[24] E. Desurvire, J. R. Simpson, and P. C. Becker, "High-gain erbium-doped traveling-wave fiber amplifier," *Opt. Lett.*, vol. 12, no. 11, pp. 888–890, 1987.

[25] G.984.5: Gigabit-capable passive optical networks (G-PON): Enhancement band, 2014.

[26] G.984.3: Gigabit-capable passive optical networks (G-PON): Transmission convergence layer specification, 2014.

[27] A. J. Tae and K. K. Hon, "All-optical gain-clamped erbium-doped fiber amplifier with improved noise figure and freedom from relaxation oscillation," *IEEE Photon. Technol. Lett.*, vol. 16, no. 1, pp. 84–86, Jan. 2004.

[28] A. Kaneko, T. Goh, H. Yamada, T. Tanaka, and L. Ogawa, "Design and applications of silica-based planar lightwave circuits," *IEEE J. Sel. Top. Quantum Electron.*, vol. 5, no. 5, pp. 1227–1236, Sep./Oct. 1999.

[29] Y. Inoue, A. Kaneko, F. Hanawa, H. Takahashi, K. Hattori, and S. Sumida, "Athermal silica-based arrayed-waveguide grating multiplexer," *Electron. Lett.*, vol. 33, no. 23, pp. 1945–1947, 1997.

[30] X. Zhao, C. F. Lam, and S. Fong, "Wavelength tunable laser," U.S. Patent 14 293 133, Jun. 2, 2014. [Online]. Available: https://patents.google.com/patent/US9240672B1/en?inventor=xiangjun+zhao.

[31] D. van Veen, W. Poehlmann, B. Farah, T. Pfeiffer, and P. Vetter, "Measurement and mitigation of wavelength drift due to self-heating of tunable burst-mode DML for TWDM-PON," in *Proc. Opt. Fiber Commun. Conf.*, San Francisco, CA, USA, 2014, Paper W1D.6.

Liang B. Du (M'08) received the B.E. degree in electrical engineering and the B.Com. degree in finance in 2007, and the Ph.D. degree in electrical engineering in 2011 from Monash University, Victoria, Australia.

He was a Research Fellow with Monash University from 2011 to 2013. In 2013, he joined Google Fiber, Mountain View, CA, USA, as a Photonics Engineer designing next-generation access networks.

Xiangjun Zhao (M'16) received the M.S. degree in optoelectronics from the Huazhong University of Science and Technology, Wuhan, China, in 1994, and the Ph.D. degree in electrical engineering from the University of Maryland Baltimore County, in 2005.

From 2007 to 2012, he worked with Infinera as a Photonics Engineer for high-speed coherent optical line-card development. Since 2012, he has been working with Google Fiber, Mountain View, CA, USA, as a Photonics Engineer, responsible for the development of next-generation DWDM passive access networks.

Shuang Yin received the B.S. degree in optical engineering from Zhejiang University, Hangzhou, China, in 2011, and the M.S. and Ph.D. degrees in electrical engineering from Stanford University, Stanford, CA, USA, in 2013 and 2016, respectively.

He joined Google Fiber, Mountain View, CA, USA, as a Photonics Engineer in 2016, and is currently responsible for the development of optical access system and network for Google Fiber. His research interests include high-speed optical access technologies, coherent transmission systems, and optical switching technologies.

Tao Zhang (M'14) received the B.S. degree in electronics and the M.S. degree in software engineering from the Huazhong University of Science and Technology, Wuhan, China, in 2006 and 2008, respectively, and the M.S. degree in electrical engineering from Southern Methodist University, Dallas, TX, USA, in 2015.

He joined Google Fiber, Mountain View, CA, USA, in 2016 as a Hardware Engineer and is currently responsible for the dense wavelength division multiplexing optical transceiver development of Google Fiber Networks. From 2013 to 2015, he worked as an IC Designer for CERN, Geneva, Switzerland, focusing on the development of the radiation-hardened transmitter ICs for the optical data-transmission links installed in the Large Hadron Collider. From 2010 to 2012, he was an ASIC Verification Engineer for LSI Corporation, Shanghai, China, and led the analog model development and chip-level verification of the ASICs for the storage products. From 2008 to 2010, he was with VIA Technologies, Beijing, China, as a Circuit Design Engineer for CPU and chipset products.

Adam E. T. Barratt received the B.A. degree in technical theatre from the University of Missouri, Columbia, MO, USA, in 2005.

From 2003 to 2011, he worked with Socket Tele-Communications as a Network Engineer. From 2011 to 2015, he worked as a Systems Engineer with ADTRAN with focus on the rural telecom market. He joined Google Fiber, Mountain View, CA, USA, in 2015 as an Access Network Engineer. In 2016, he moved to Google Fiber's network architecture team as a Senior Broadband Access Architect, responsible for systems designs related to physical and logical aggregation of end users and provisioning systems.

Joy Jiang received the B.S. degree in precision instruments from Tsinghua University, Beijing, China, the M.S. degree in mechanical engineering from Washington State University, Pullman, WA, USA, and the Ph.D. degree in mechanical engineering from the University of California, Berkeley, CA, USA.

She worked with JDSU as a Product Line Manager and a Market Group Leader, responsible for starting the Fibre Channel over Ethernet product line and owning Fibre Channel and Ethernet product lines as well. In 2013, she joined Google Fiber, Mountain View, CA, USA, as a Technical Program Manager. She manages various innovative development projects such as LRWR-PON, the super TWDM-PON network that was developed by Google Fiber.

Daoyi Wang received the B.S. and Ph.D. degrees in optical engineering from Tsinghua University, Beijing, China, in 1997 and 2001, respectively.

From 2001 to 2009, he worked with Alliance Fiber Optic Products, Inc., and was responsible for micro-optic device development. From 2009 to 2014, he worked with Infinera Inc. as an Optical Engineer for high-speed optical line module development and NPI. He joined Google Inc., Mountain View, CA, USA, as a Hardware Engineer in 2015. His research interests include advanced optical technologies and optical interconnect for data center application.

Junyan Geng received the B.S. degree from the University of California, Los Angeles, CA, USA, in 2015, and the M.S. degree from Columbia University, New York, NY, USA, in 2017, both in electrical engineering.

She was interning with Google Fiber, Mountain View, CA, USA, as a Hardware Engineer in 2015, focusing on test automation and optical components evaluation. In 2017, she joined Waymo, Mountain View, CA, USA, as a Hardware Engineer. Her work currently includes signal integrity simulation and design validation of self-driving car's system components.

Claudio DeSanti received the Bachelor of Science cum laude in computer engineering from the University of Pisa, Pisa, Italy, in 1995, and the Ph.D. degree in computer engineering from Scuola Superiore di Studi Universitari e di Perfezionamento S. Anna, Pisa, Italy, in 2000.

From 2000 to 2017, he worked with Cisco Systems up to the Fellow level. He contributed to the development and success of many Cisco products, including Cisco's UCS, Cisco's Nexus 7K and 5K, Cisco's MDS, and Cisco's Catalyst switches. He is the Inventor of Fibre Channel over Ethernet and many other Storage Networking technologies. He joined Google, Mountain View, CA, USA, in 2017 as a Senior Network Architect Lead. He is highly recognized in Standards Bodies and industry associations, such as INCITS T11, IEEE 802.1 and 802.3, and IETF. He has been the Conference Chairman of Ethernet Technology Summit, the Vice Chairman of the INCITS T11 Technical Committee, the Chairperson of multiple working groups, and a Technical Editor of different standards, including IEEE 802.1Qbb. He is the author of several patents and recipient of four INCITS technical awards.

Cedric F. Lam (SM'07) received the B.Eng. degree (with first-class honors) in electrical and electronic engineering from the University of Hong Kong, Pokfulam, Hong Kong, in 1993, and the Ph.D. degree in electrical engineering from the University of California, Los Angeles, CA, USA, in 1999.

From 1999 to 2002, he worked with AT&T Labs – Research as a Senior Technical Staff Member. From 2002 to 2009, he was a Chief System Architect with OpVista, leading the development of an ultra-dense DWDM transport system. He joined Google, Mountain View, CA, USA, in 2009 as a Datacenter Network Architect. In 2010, he co-founded the Google Fiber program and is currently the Engineering Director with Google Fiber, responsible for network architecture and network technology development.

Dr. Lam is a Fellow of the Optical Society of America.